

# Synthetic-Bioinformatic Natural Product Antibiotics with Diverse Modes of Action

John Chu, Bimal Koirala, Nicholas Forelli, Xavier Vila-Farres, Melinda A. Ternei, Thahmina Ali, Dominic A. Colosimo, and Sean F. Brady\*



Cite This: *J. Am. Chem. Soc.* 2020, 142, 14158–14168



Read Online

ACCESS |



Metrics & More

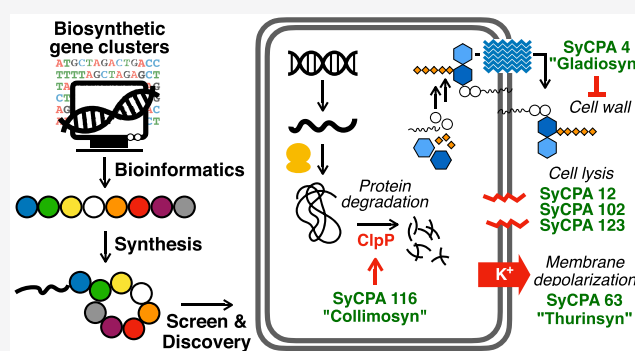


Article Recommendations



Supporting Information

**ABSTRACT:** Bacterial natural products have inspired the development of numerous antibiotics in use today. As resistance to existing antibiotics has become more prevalent, new antibiotic lead structures and activities are desperately needed. An increasing number of natural product biosynthetic gene clusters, to which no known molecules can be assigned, are found in genome and metagenome sequencing data. Here we access structural information encoded in this underexploited resource using a synthetic-bioinformatic natural product (syn-BNP) approach, which relies on bioinformatic algorithms followed by chemical synthesis to predict and then produce small molecules inspired by biosynthetic gene clusters. In total, 157 syn-BNP cyclic peptides inspired by 96 nonribosomal peptide synthetase gene clusters were synthesized and screened for antibacterial activity. This yielded nine antibiotics with activities against ESKAPE pathogens as well as *Mycobacterium tuberculosis*. Not only are antibiotic-resistant pathogens susceptible to many of these syn-BNP antibiotics, but they were also unable to develop resistance to these antibiotics in laboratory experiments. Characterized modes of action for these antibiotics include cell lysis, membrane depolarization, inhibition of cell wall biosynthesis, and ClpP protease dysregulation. Increasingly refined syn-BNP-based explorations of biosynthetic gene clusters should allow for more rapid identification of evolutionarily inspired bioactive small molecules, in particular antibiotics with diverse mechanism of actions that could help confront the imminent crisis of antimicrobial resistance.



## INTRODUCTION

Many antibiotics in clinical use today are either molecules originally discovered from bacterial fermentation broths or synthetic variants of these metabolites.<sup>1</sup> Key to the tremendous success of natural products in antibiotic discovery pipelines is the amazing diversity of ways by which they have evolved to inhibit bacterial growth.<sup>2</sup> However, despite the success of culture-dependent antibiotic discovery programs, large genome and metagenome sequencing efforts indicate that we have accessed only a small fraction of the bacterial biosynthetic potential present in nature.<sup>3</sup> In fact, sequenced biosynthetic gene clusters that do not appear to correspond to any known metabolites far exceed the number of bacterial natural products that have been isolated and structurally characterized.<sup>3c,4</sup> The development of new methods for converting this untapped reservoir of genetic information into chemical structures should help to repopulate antibiotic discovery pipelines with new molecules that function by diverse modes of action.<sup>5</sup> Toward this end, we have been exploring a pipeline that does not rely on the complex *in vivo* processes of transcription, translation, and enzyme catalysis to produce natural products for sequenced gene clusters (Figure 1a). In this purely *in vitro*

approach, which we have termed synthetic-bioinformatic natural products (syn-BNPs), the structures of natural products encoded by biosynthetic gene clusters are predicted bioinformatically, and the resulting predictions are then chemically synthesized to generate libraries of molecules that are inspired by nature.<sup>6</sup> The syn-BNP approach is not expected to generate exact copies of natural products but instead provide libraries of biomimetic natural product congeners that should be enriched for evolutionarily selected biological activities.

Although bacteria use numerous biosynthetic strategies to generate structurally diverse antibiotics, among the most productive is the ribosome-independent biosynthesis of short linear and cyclic peptides by nonribosomal peptide synthetases (NRPSs).<sup>7</sup> Algorithms for predicting the peptide products of

Received: April 21, 2020

Published: July 22, 2020



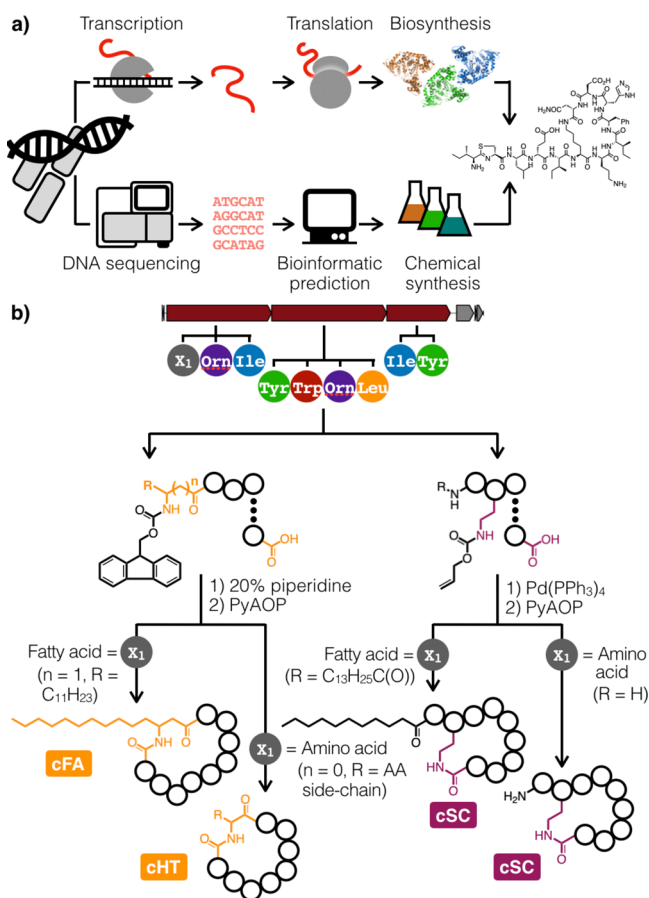


**Figure 1.** (a) In biological systems, enzymatic machinery produces an NRP based on the information encoded within biosynthetic genes. In a syn-BNP approach, chemical synthesis produces a close structural mimic based on predictions made by bioinformatic algorithms. (b) We devised a synthetic scheme to allow each predicted peptide sequence to be cyclized in two ways at the desired position.

NRPS gene clusters as well as methods for synthesizing peptides are well-established, making these gene clusters appealing targets for syn-BNP discovery efforts. Although the majority of characterized nonribosomal peptides are cyclic, early syn-BNP studies largely focused on the synthesis of simple linear peptides.<sup>6a–d</sup> To better mimic natural products, we expanded our predictive and synthetic efforts to include NRPS-inspired cyclic structures.<sup>6e</sup> Here we report on the discovery of nine new syn-BNP cyclic peptide antibiotics (SyCPAs) that collectively have multiple modes of actions, show both narrow and broad spectra of activity against antibiotic-resistant pathogens, and, in many cases, did not easily develop resistance in the laboratory. Our results suggest that the application of increasingly elaborate syn-BNP methods to cryptic biosynthetic gene clusters is likely to be a rewarding strategy for identifying naturally inspired, bioactive molecules, in particular, mechanistically diverse antibiotics that could help repopulate and diversify antibiotic discovery pipelines.

## METHODS

**Chemical Reagents, Consumables, and Instruments.** Pre-loaded 2-chlorotrityl resins for peptide syntheses were purchased from Matrix Innovation, Inc. (Quebec, Canada). Reagents for solid-phase peptide synthesis (SPPS), that is, PyAOP ((7-azabenzotriazol-1-yloxy) tripyrrolidinophosphonium hexafluorophosphate), PyBOP ((benzotriazole-1-yloxy) tripyrrolidinophosphonium hexafluoro-

phosphate), HATU (O-(7-Azabenzotriazol-1-yl)-N,N,N',N'-tetramethyluronium hexafluorophosphate), and Cl-HOBt (6-chloro-1-hydroxy benzotriazole), were purchased from P3 BioSystems (Louisville, KY). Standard N-Fmoc amino acid building blocks were purchased from P3 BioSystems and Chem-Impex International (Wood Dale, IL), and building blocks with allyloxycarbonyl (Alloc) protected side-chains were purchased from Ark Pharm, Inc. (Arlington Heights, IL) and Chempep, Inc. (Wellington, FL). (D/L)-N-Fmoc-3-aminotetradecanoic acid was purchased from Chemeliva Pharmaceutical Co. (Chongqing, China). MTT [3-(4,5-dimethyl-thiazol-2-yl)-2,5-diphenyltetrazolium bromide], tetradecanoic acid, Pd(PPh<sub>3</sub>)<sub>4</sub> (tetrakis(triphenylphosphine) palladium (0)), and solid-phase extraction (SPE) C-18 cartridges were purchased from Sigma-Aldrich (St. Louis, Missouri). A 12-position SPE vacuum manifold was manufactured by WXIntl (Rowland Heights, CA) and purchased on eBay. Fluorescent dyes SYTOX Green and DISC<sub>3</sub>(S) (3,3'-dipropylthiadicarbocyanine iodide) were purchased from ThermoFisher Scientific (Waltham, MA), and the assay results were recorded using a SpectraMax M2e (Molecular Devices, San Jose, CA). Peptide purification was performed on an XBridge Prep C-18 column (Waters Corporation, Milford, MA) using a 1200 HPLC system (Agilent Technologies, Santa Clara, CA). LCMS was performed on a Waters Acquity UPLC M-class system. All other reagents, solvents, and consumables were purchased from VWR International (Radnor, PA). The ClpP protease assay kit was purchased from ProFoldin (Hudson, MA), and a Tecan Infinite M Nano+ plate reader (Morrisville, NC) was used to measure protease degradation.

**Microbes, Cell Line, and Growth Media.** Bacterial strains and growth conditions appear in Table S2. Growth media, including Luria–Bertani (LB), brain heart infusion (BHI), and tryptic soy broth (TSB), for microbes were purchased as premade powders from Becton Dickinson (Franklin Lakes, NJ). Aerobic bacterial cultures were grown shaken (200 rpm), and cultures of facultative aerobic bacteria (*Streptococcus* and *Lactobacillus* species) were grown statically in an anaerobic chamber. Primary screening of Syn-BNP cyclic peptides was performed on bacteria embedded solid media [LB supplemented with 1.5% (w/v) agar] grown statically at 30 °C.

**Syn-BNP Peptide Sequence Prediction.** High quality complete bacterial genomes present in GenBank as of December 2014 (~3000) at the time this project was initiated were analyzed by using antiSMASH bacterial version 2.0.<sup>8</sup>

**SPPS and Peptide Cyclization.** All target peptides were produced by standard Fmoc (fluorenylmethoxycarbonyl) based solid-phase synthesis on 2-chlorotrityl resins using standard amino acid building blocks. To facilitate side-chain cyclization reactions, serine and threonine nucleophiles were replaced with 2,3-diaminopropionic acid, an isosteric residue that contains a more reactive nitrogen nucleophile. Similarly, 3-aminomyristic acid was used as the fatty acid for generating N-acylated peptides. The side-chain amines on residues used as cyclization nucleophiles (e.g., diaminopropionic acid, ornithine, or lysine) were protected with an allyloxycarbonyl group to permit palladium-catalyzed differential deprotection. The 3-amino-myristic acid in N-acylated peptides as well as the N-terminus of nonacylated peptides was protected with Fmoc to permit differential deprotection with piperidine. Syn-BNP cyclic peptides for primary screening were synthesized from their linear counterparts purchased as on-resin crude materials from Ontores Biotechnologies, Inc. (Hangzhou, China) and Tahepna Biotechnologies, Co. (Hangzhou, China). Peptides used in validation and follow up studies were synthesized in-house either through manual synthesis or using a Biotage Alstra Initiator-plus automated microwave synthesizer (Charlotte, NC). Syntheses were performed as described previously<sup>6e</sup> with the exception that tetradecanoic acid and N-Fmoc-3-amino-tetradecanoic acid were used in the N-acylation of cSC and cFA peptide designs, respectively.

**Peptide Purification: Solid-Phase Extraction.** C18 cartridges were mounted on a vacuum manifold that enables the purification of up to 12 peptides in parallel. Crude material from cyclization reactions was solubilized in the minimal amount of methanol (MeOH) and mixed with an equal volume of water. The resulting

precipitate/suspension was immediately loaded onto a C18 cartridge that had been prewashed with MeOH (10 mL) and water (10 mL). The cartridge was washed with 50% MeOH (10 mL), acidified 50% MeOH (1% v/v formic acid), eluted with 100% MeOH, and the eluted MeOH fraction was dried by using a speedvac. Global deprotection was accomplished by treating the cyclic peptides with trifluoroacetic acid (TFA) containing water and triisopropylsilane [2.5% (v/v) of each] at room temperature for 2 h. Liquid chromatography coupled with low-resolution mass spectrometry (LCMS) was used to verify the presence of the desired Syn-BNP cyclic peptide once TFA had evaporated. This crude material was dissolved in DMSO (12.8 mg/mL) and used directly in primary antimicrobial screening.

**Cyclic Peptide Purification: HPLC.** Crude Syn-BNP cyclic peptides that showed antimicrobial activity were purified on a XBridge Prep C18 HPLC column (130 Å, 5 μm, 10 × 250 mm<sup>2</sup>) using a dual solvent system (A/B: water/acetonitrile, supplemented with 0.1% v/v of formic acid). Most peptides were eluted 35 to 75% B. Pure peptides were confirmed by HRMS and MS/MS analyses, dissolved in DMSO at 12.8 mg/L for MIC measurements and mechanism of action studies. Diastereomers of antibiotic hits (if separable) were tested as separate entities, and the more active isomer was used in MOA studies.

**Primary Antimicrobial Screening.** Single colonies of bacteria were inoculated in LB broth and grown overnight at 200 rpm in a shaking incubator at 37 °C. The overnight culture was used to reinoculate fresh LB broth (1/200×), grown to late log phase (OD<sub>595</sub> ≈ 1.0), and mixed with molten LB/agar [1.5% (w/v), 50 mL] at 55 °C. The mixture was poured onto a Petri dish (150 × 15 mm<sup>2</sup>) and allowed to cool down to room temperature inside a laminar flow hood. DMSO solutions of 4 μL of each Syn-BNP cyclic peptides at 12.8 and 4.27 μg/μL were spotted directly on solidified LB/agar embedded with bacteria. Alongside Syn-BNPs, three known antibiotics (carbenicillin, chloramphenicol, kanamycin) and DMSO were used as the positive and negative controls, respectively. Once the DMSO droplets have been absorbed into the solid media, the Petri dishes were incubated statically at 30 °C for 18 h. On the following day, the Petri dishes were visually inspected, and each Syn-BNP was given a semiquantitative score on the scale of 0 (inactive) to 3 (potent) based on the size and clarity of its corresponding growth inhibition zone.

**Resynthesis of Nine Active SyCPAs. Solid-Phase Peptide Synthesis.** 2-Chlorotriethyl resin preloaded with the first amino acid (0.2 g, 0.455 mmol/g) was swollen in DCM for 30 min at room temperature and drained under vacuum. The resin was then washed with DMF (3 mL, 4×). Couplings proceeded with the addition of two molar equivalents (relative to resin loading) of the respective Fmoc-protected amino acids that were activated by HATU (2 equiv) and diisopropylethylamine (DIEA, 2 equiv) in DMF (3 mL). Reactions were allowed to proceed at room temperature for 1 h with occasional swirling. The resin was then drained under vacuum and washed with DMF (3 mL, 4×). Fmoc removal was carried out by treatment with 20% piperidine in DMF for 7 min with occasional swirling (2 mL, 2×). After deprotection, resins were washed with DMF (3 mL, 4×). Fatty acids, *N*-Fmoc-3-aminotetradecanoic acid, or myristic acid (2 equiv), as predicted, was activated and coupled to the *N*-termini of the resin bound synthetic peptides using the same procedure.

**Alloc Deprotection for Side-Chain Cyclized Peptides.** SyCPA 2, SyCPA 4, SyCPA 12, and SyCPA 63 were cyclized between the *C*-terminus of the peptide and a side chain amino group. Alloc deprotection of the amino acid side chain used for cyclization was performed by first washing resin bound linear peptides with dry DCM (3 mL, 4×) and then flushing with argon. Phenylsilane (15 equiv) and Pd(PPh<sub>3</sub>)<sub>4</sub> (0.5 equiv) were dissolved in dry DCM (5 mL) at room temperature under anhydrous argon and added to the resin. This mixture was allowed to react for 2 h with occasional swirling. After 2 h, the resin was washed with 10% sodium diethyldithiocarbamate trihydrate in DMF (5 mL, 5×) to remove the palladium, followed by washes with DMF (3 mL, 4×) and DCM (5 mL, 5×). The synthetic linear peptides were then cleaved from the resin (see below).

**Fmoc Removal for Fatty Acid Cyclized Peptides.** SyCPA 102, SyCPA 116, SyCPA123, and SyCPA144 were cyclized between the *C*-terminus of the peptide and the 3-amino group on the fatty acid (3-aminotetradecanoic acid). The *N*-Fmoc group was removed using 20% piperidine in DMF as described above. The synthetic linear peptides were then cleaved from the resin (see below).

**Fmoc Removal for Head-to-Tail Cyclized Peptide.** SyCPA 153 was cyclized between its *C*- and *N*-termini. The *N*-terminal Fmoc group was removed using 20% solution in DMF as described above. The synthetic linear peptide was then cleaved from the resin (see below).

**Cleavage and Cyclization.** The resin bound linear peptides were cleaved from the resin to perform peptide cyclization. The resin was treated with 1% TFA in DCM (2 mL, 10×), immediately neutralized with 10% DIEA in DCM, and then air-dried overnight. The cleaved linear peptides were dissolved in DMF (40 mL). PyAOP (7 equiv) and DIEA (15 equiv) were added at room temperature, and the reaction was allowed to proceed for 1 h. DCM (50 mL) was added to the cyclized peptide and washed repeatedly with 1% formic acid in water (5 mL, 10×). The extracted peptide was air-dried overnight.

**Global Deprotection.** The dried cyclic peptides were transferred into 50 mL falcon tubes and mixed with 3 mL of TFA containing 2.5% (v/v) water and 2.5% (v/v) triisopropylsilane. Global deprotections were carried out at room temperature for 3 h with occasional swirling. Diethyl ether and hexane were mixed 1:1 (45 mL in total), cooled to −20 °C, and then added to the above TFA treated peptides. Cyclic peptides were allowed to precipitate at −20 °C for 20 min and collected by centrifugation (2500g, 5 min). Crude peptide pellets were dissolved in 5 mL of methanol and dried overnight in a speed-vac.

**Peptide Purification.** Dried crude cyclic peptides were dissolved in 50% methanol (4 mL). They were then HPLC purified in 0.5 mL portions using a Waters XBridge prep C18 column (5 μm, 10 × 250 mm<sup>2</sup>) and a 40 min linear gradient from 35 to 75% acetonitrile supplemented with 0.1% (v/v) of formic acid. Peptide purity and identity were confirmed by UPLC, HRMS (Table S3), tandem MS (Figure S3), and <sup>1</sup>H NMR (Figures S4–S12).

**MIC Determination.** Standard susceptibility assays were performed in the appropriate growth medium in 96-well microtiter plates to determine the minimum inhibitory concentration (MIC) by the broth microdilution method in accordance to protocols recommended by Clinical and Laboratory Standards Institute.<sup>9</sup> For polymyxin-supplemented assays, the MIC of polymyxin against a bacterium was first determined (1× MIC). The growth medium for setting up a MIC assay was then supplemented with polymyxin at 1/4× MIC of each respective bacteria. The measured MICs were as follows: *E. coli* DH5α (0.0625 μg/mL), *K. pneumoniae* and *P. aeruginosa* (0.15 μg/mL), *A. baumannii* (0.3 μg/mL), and *E. cloacae* (2 μg/mL). Note that the *E. cloacae* ATCC 13047 strain we used was not susceptible to polymyxin (MIC > 64 μg/mL). These supplemented growth media were then used in a standard broth microdilution to determine the polymyxin-supplemented MIC of each antibiotic hit. All assays were done at least in duplicate (*n* = 2).

**Membrane Depolarization Assay.** Membrane depolarization assays were done in a 384-well plate, and all stock solutions were prepared in Dulbecco's phosphate buffer saline (PBS). An overnight bacterial culture was harvested by centrifugation, washed twice with PBS, and resuspended in PBS (OD<sub>595</sub> ≈ 0.4). Cell suspension (10 μL) and 20 μM DiSC<sub>3</sub>(5) (5 μL) were added to PBS (15 μL) and incubated in the dark at room temperature for 15 min. Potassium chloride (2 M, 5 μL) was added and incubated for another 15 min. This mixture was then transferred into a 384-well microtiter plate, and its fluorescence intensity was recorded continually at 3 s intervals (*E*<sub>λ</sub>/*E*<sub>m</sub> 643/675 nm). Once the signal had stabilized, which takes approximately 3 to 5 min, Syn-BNP antibiotics were added and immediately mixed by manual pipetting without stopping recording. The final mixture is a PBS solution containing DiSC<sub>3</sub>(5) (1 μM), KCl (100 mM), bacteria (OD<sub>595</sub> ≈ 0.04), and antibiotics at 1× MIC against the bacteria of interest. Gramicidin and DMSO were used as the positive and negative controls, respectively. All assays were done

in duplicate ( $n = 2$ ); a representative recording for each Syn-BNP is shown in either Figure 4c or d.

**Membrane Lysis Assay.** Membrane lysis assays were done in disposable plastic cuvettes, and all stock solutions were prepared in LB broth. An overnight bacterial culture was harvested by centrifugation and resuspended in fresh LB ( $OD_{595} \approx 0.4$ ). SYTOX Green ( $15 \mu\text{M}$ ,  $100 \mu\text{L}$ ) was added to the cell suspension ( $900 \mu\text{L}$ ) and incubated in the dark at room temperature for 10 min. Fluorescence intensity of the mixture was recorded continually at 2 s intervals ( $E_x/E_m$  488/523 nm). Once the signal had stabilized, which takes approximately 3 to 5 min, syn-BNP antibiotic as a  $12.8 \text{ mg/mL}$  DMSO solution was added and immediately mixed by manual pipetting without stopping the recording. The final mixture is a LB solution containing SYTOX ( $1.5 \mu\text{M}$ ), bacteria ( $OD_{595} \approx 0.04$ ), and antibiotics at  $1\times$  MIC against the bacteria of interest. Daptomycin supplemented with  $10 \text{ mM}$  calcium chloride ( $\text{CaCl}_2$ ) and DMSO were used as the negative control and positive controls. Data were presented as the relative intensity with respect to the average fluorescence signal prior to the addition of the antibiotic. All assays were done in duplicate ( $n = 2$ ); a representative recording for each Syn-BNP is shown in either Figure 4c or d.

**Lipid II Precursor Accumulation Assay.** A single bacterial colony was inoculated into LB and grown overnight at 200 rpm in a shaking incubator at  $37^\circ\text{C}$ . On the following day, the overnight culture was used to reinoculate fresh LB broth ( $1/200\times$ ) and grown to mid log phase ( $OD_{595} \approx 0.5$ ). Chloramphenicol was added to  $1 \text{ mL}$  of mid log phase culture and incubated at  $37^\circ\text{C}$  for 20 min at 200 rpm. Antibiotics of interest were added at  $20 \mu\text{g/mL}$  and incubated for another 60 min. Cells were collected by centrifugation, resuspended in  $30 \mu\text{L}$  of water, and then incubated in boiling water for 15 min. The boiled suspension was centrifuged at  $15\ 000g$ , and the supernatant was analyzed by LCMS. Vancomycin and DMSO were used as the positive and negative controls, respectively. All assays were done in duplicate ( $n = 2$ ); a representative trace for each Syn-BNP was shown in Figure 5a.

**Cytotoxicity Assessment.** HeLa cells were grown in Dulbecco's modified Eagle medium (DMEM) supplemented with penicillin ( $10 \text{ units/mL}$ ), streptomycin ( $10 \text{ units/mL}$ ),  $L$ -glutamate ( $2 \text{ mM}$ ), and heat-inactivated fetal bovine serum ( $10\% \text{ v/v}$ ) at  $37^\circ\text{C}$  in a  $5\% \text{ CO}_2$  atmosphere. HeLa cells were seeded into 384-well plates ( $500 \text{ cells per well}$ ) and incubated in DMEM at  $37^\circ\text{C}$  with  $5\% \text{ CO}_2$  for 16 h to allow cells to adhere. The  $OD_{570}$  readings were used to calculate relative growth (%) based on the positive ( $2 \mu\text{M}$  Taxol,  $0\%$ ) and negative (DMSO,  $100\%$ ) controls. The cytotoxicity assay was performed in quadruplicate ( $n = 4$ ) and analyzed according to protocol reported previously.<sup>6c</sup>

**Resistant Mutant Selection and SNP Identification.** Resistant mutants were raised as reported previously.<sup>6a</sup> Briefly, a single bacterial colony was inoculated into LB and grown overnight at 200 rpm in a shaking incubator at  $37^\circ\text{C}$ . A portion of the overnight culture containing approximately  $10^9$  cells was diluted ( $1/100\times$  to  $1/400\times$  fold) into LB containing the antibiotic of interest at  $2.5\times$  of its MIC. The resulting mixture was distributed into microtiter plates at  $200 \mu\text{L}$  per well. After incubating statically at  $30^\circ\text{C}$  for 12 to 18 h, colonies that appeared were transferred into fresh LB containing the same concentration of antibiotic. In a second round of selection, these cultures were grown at  $30^\circ\text{C}$  for an additional 12 to 18 h. Mature cultures were struck for singles on LB/agar free of antibiotics. The MIC of 12 to 36 individual colonies was then tested using the standard microtiter dilution method described above. DNA was extracted from cultures of colonies that showed elevated MIC, and the resulting DNA was sequenced using MiSeq Reagent Kit V3 (MS-102–3003, Illumina). DNA extraction and next generation sequencing were performed as reported previously. Single-nucleotide polymorphisms (SNPs) were identified using SNIPPY (<http://github.com/tseemann/snippy>) by mapping MiSeq reads to the reference genome of *S. aureus* USA300\_FPR3757 (RefSeq assembly accession: GCF\_000013465.1).

## RESULTS AND DISCUSSION

**Bioinformatic Analysis, Design, and Synthesis of NRPS-Inspired Cyclic Syn-BNPs.** Nonribosomal peptides are produced by modular assembly line-like enzymes. In canonical systems, each module incorporates a single amino acid into a growing peptide. Detailed bioinformatic analyses of functionally characterized NRPS gene clusters have led to the development of algorithms that use protein sequence data to predict the identity and order of the amino acid building blocks encoded by a gene cluster.<sup>8,10</sup> To generate syn-BNP targets, we bioinformatically analyzed large ( $\geq 5$  adenylation domains) NRPS gene clusters found in  $\sim 3000$  complete bacterial genomes present in GenBank.<sup>11</sup> For each gene cluster, we predicted the peptide it encoded using three different prediction tools.<sup>10</sup> We excluded from further analysis any gene clusters that were predicted to encode known nonribosomal peptides, a large number of tailoring enzymes, or residues that did not have a consensus prediction across algorithms. We also removed from further analysis those gene clusters that did not appear to follow a canonical colinear organization pattern. From the remaining NRPS gene clusters, we selected 96 linear peptide predictions to serve as the basis of our cyclic syn-BNP targets (Table S1).

The majority of characterized nonribosomal peptides are cyclized through their C-termini, and therefore, we focused our synthetic efforts on generating C-terminally cyclized syn-BNPs. Monocyclic nonribosomal peptides that are cyclized through the C-terminal carboxylate can largely be grouped into three distinct categories based on the nucleophile that is used in the cyclization reaction. The carboxylate can react with either an amino acid side-chain, the N-terminus of the peptide, or in the case of N-acylated peptides, a nucleophile on the fatty acid. While bioinformatically predicting the specific nucleophile used for cyclization remains challenging,<sup>12</sup> an analysis of characterized cyclic nonribosomal peptides revealed the following trends:<sup>6e,13</sup> (1) when more than one potential side-chain nucleophile is present, nonribosomal peptides are most often cyclized through the residue that yields the largest macrocycle, (2) fatty acid cyclization most commonly occurs through beta-oxidation of the lipid, and (3) the vast majority of nonribosomal peptide macrocycles contain four or more amino acid residues ( $n \geq 4$ ). We used these observations to guide the design of sets of differential cyclic syn-BNP targets for each linear nonribosomal peptide prediction (Figure 1b). Specifically, when a nonribosomal peptide was predicted to be N-acylated with a fatty acid, the corresponding syn-BNP peptide was cyclized through either the  $\beta$ -heteroatom of the fatty acid (cFA, Figure 1b) or the nucleophilic amino acid side-chain closest to the N-terminus (cSC, Figure 1b). Alternatively, when no fatty acid was predicted to be present at the N-terminus, the syn-BNP peptide was cyclized either head-to-tail (cHT, Figure 1b) or through a nucleophilic side-chain (cSC, Figure 1b). Finally, peptides inspired by NRPS gene clusters that were predicted to encode products without a nucleophilic side-chain capable of forming a macrocycle of at least four amino acids were only cyclized either head-to-tail or through their fatty acids. Using this general scheme, we targeted the synthesis of 171 syn-BNPs that were inspired by our 96 linear peptide predictions. Each cyclization reaction was partitioned over a C-18 solid-phase extraction cartridge to obtain a semipure synthetic cyclic peptide. The desired target mass was identified in 157 (92%) cases (Table S1). Fractions containing

the target masses were dried *in vacuo*, resuspended in DMSO, and used directly for bioactivity screening.

**Syn-BNP Screening for Antibiosis.** Nonribosomal peptides display a wide variety of bioactivities, but they have offered their greatest utility as antibiotics.<sup>14</sup> To identify antibacterial active syn-BNPs, we screened each fraction containing the mass of a target syn-BNP cyclic peptide against *Bacillus subtilis*, *Escherichia coli*, and the ESKAPE pathogens. The ESKAPE pathogens represent the bacteria most commonly associated with antibiotic-resistant nosocomial infections: *Enterococcus faecium*, *Staphylococcus aureus*, *Klebsiella pneumoniae*, *Acinetobacter baumannii*, *Pseudomonas aeruginosa*, and *Enterobacter cloacae*.<sup>15</sup>

In our initial screen, semipure peptides were spotted on solid growth media seeded with each bacterium. After the bacterial lawns matured, a semiquantitative score on a scale from 0 (inactive) to 3 (clear growth inhibition zone) was assigned to each cyclic peptide (Figure 2a). Syn-BNPs scoring a “3” against

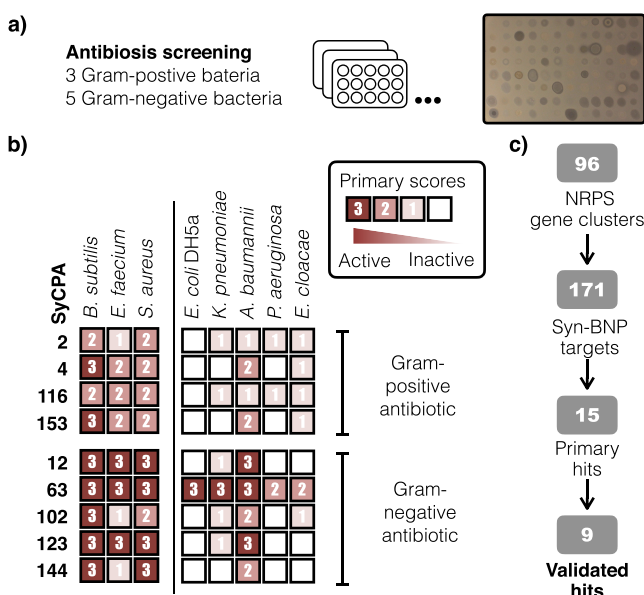


**Figure 2.** (a) Syn-BNPs were screened against a panel of bacteria to identify new antibiotics. This panel included model Gram-positive and Gram-negative bacteria (*B. subtilis* and *E. coli*, respectively) as well as the ESKAPE pathogens. (b) Each Syn-BNP was given a semiquantitative score for its activity against each bacterium that ranged from 0 (inactive) to 3 (most potent) based on the size of its zone of growth inhibition. (c) A total of 171 Syn-BNP cyclic peptides were synthesized based on bioinformatic predictions of 96 NRPS gene clusters. We identified 15 primary hits from this syn-BNP collection. Nine hits were validated upon resynthesis.

any bacterium or having a combined score of 8 or higher across all pathogens were regarded as primary hits. In total, we identified 15 fractions that reached one or both thresholds. Syn-BNPs were purified by HPLC from the fractions associated with each primary hit and then reassayed for antibacterial activity (Figure 2b). Once purified, nine primary hits showed an MIC of  $\leq 8$   $\mu\text{g}/\text{mL}$  against at least one bacterium in our panel. We called these validated hits syn-BNP cyclic peptide antibiotics (SyCPAs) and considered them our final set of active compounds (Figure 3). Many previously characterized natural product antibiotics have similar single-digit  $\mu\text{g}/\text{mL}$  MICs, indicating that even though syn-BNPs are unlikely to be perfect copies of evolutionary optimized natural

products, they can have potencies that are comparable to antibiotics produced using biosynthetic machinery.

**Spectrum of Activity of SyCPAs.** Four SyCPAs are Gram-positive specific antibiotics and five show activity against at least one Gram-negative bacterium (Figure 4a). Almost all SyCPAs are active against at least one antibiotic-resistant ESKAPE pathogen. Among the Gram-positive active antibiotics, we see distinct activity patterns. SyCPA 4 and 153 are mostly active against *B. subtilis*, while SyCPA 2 and 116 show broader Gram-positive activity. Broad-spectrum SyCPAs range from being active against a number of the Gram-negative bacteria we tested (SyCPA 63) to only being active against *A. baumannii* (SyCPA 123 and 144). When assayed for cytotoxicity against HeLa cells using the 3-(4,5-dimethylthiazol-2-yl)-2,5-diphenyl-tetrazolium (MTT) metabolic activity assay (Figure 4b), SyCPA 2 and 116 were the only peptides that showed significant toxicity ( $\text{IC}_{50}$  16 and 11  $\mu\text{g}/\text{mL}$ , respectively), indicating that most SyCPAs are not general cytotoxins but are instead specifically antibiotics.

All nine SyCPAs were designed based on biosynthetic gene clusters that, to the best of our knowledge, have not been previously associated with any natural products and their structures do not closely resemble any natural products deposited in the Dictionary of Natural Products or SciFinder databases (Figure S2).<sup>13,16</sup> These SyCPAs range from 5 to 13 amino acids in length and contain 18 to 39-membered macrocycles (Figure 3). Representatives of all three cyclization modes we employed are found among our final hits. The largest peptide, SyCPA 153, is the lone head-to-tail macrocycle (cHT). Four peptides each belong to the other two types of cyclic modes, that is, cyclization through the fatty acid (cFA, SyCPA 102, 116, 123, and 144) and cyclization through a nucleophilic side-chain (cSC, SyCPA 2, 4, 12, and 63). As opposed to being dominated by metabolites from Actinobacteria, which has been the most productive source of antibiotics from fermentation-based discovery efforts, the majority of SyCPAs were inspired by biosynthetic gene clusters found in the genomes of Proteobacteria and Firmicutes: 4 from Proteobacteria, 3 from Firmicutes, and 2 from Actinobacteria. As the syn-BNP approach focuses on individual biosynthetic gene clusters and not entire organisms, it is not biased by the need for a bacterium to be “biosynthetically rich” to justify its inclusion into the screening platform and therefore more likely to provide access to molecules inspired by “gene cluster poor” taxa that might otherwise be deprioritized in natural product screening programs.

**Mode of Action Studies.** Although known cyclic peptide antibiotics have diverse modes of action, they have frequently been found to either inhibit cell wall biosynthesis by binding intermediates in this biosynthetic pathway or cause membrane disruption through depolarization or cell lysis.<sup>17</sup> We therefore tested each SyCPA for these common modes of action using three discrete assays: SYTOX fluorescence (cell lysis), 3,3'-dipropylthiadicarbonycyanine iodide (DiSC<sub>3</sub>(5)) fluorescence (membrane depolarization), and UDP-MurNAc-pentapeptide accumulation (inhibition of cell wall biosynthesis).

**Cell Lysis by the Broad Spectrum SyCPAs 12, 102, and 123.** Cell lysis was assessed using the nucleic acid binding dye SYTOX. Antibiotics were tested for lytic activity against *S. aureus* unless they were significantly more active against *B. subtilis*, in which case *B. subtilis* was used (Figure 4c,d). At 4 $\times$  their MICs, three broad spectrum antibiotics, SyCPA 12, 102,

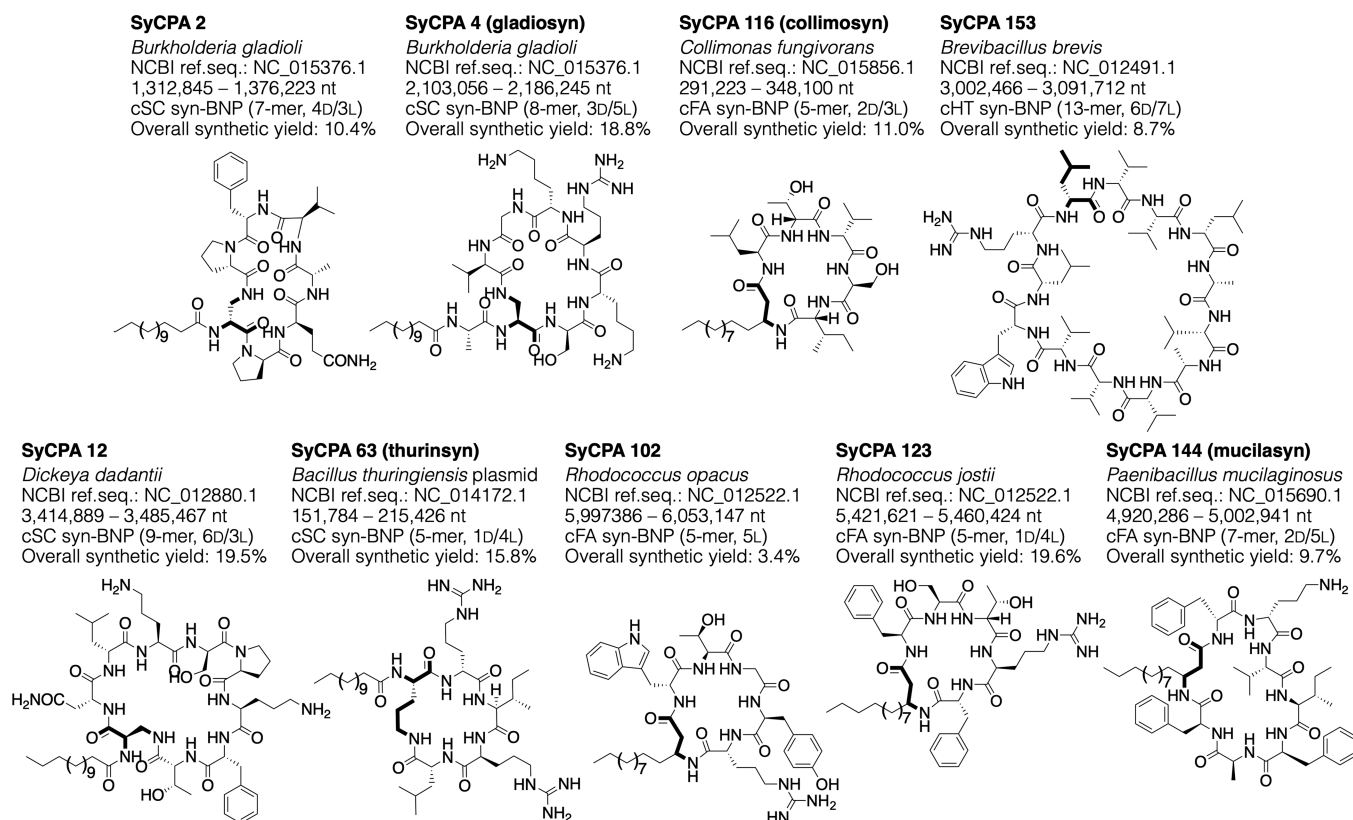


**Figure 3.** Structures of validated SyCPAs, key features of the NRPS gene cluster from which each was predicted, and their respective overall synthetic yields are shown above. Bold bonds indicate the site of cyclization.

and **123**, induced SYTOX fluorescence, indicating that they induce cell lysis. All three of these antibiotics contain positively charged residues. Cationic peptide antibiotics are a structurally diverse class of natural products that commonly function by interference with the cytoplasmic membrane barrier.<sup>18</sup> They have attracted growing interest in recent years because they often exhibit activity against antibiotic resistant Gram-negative pathogens and show low rates of resistance.<sup>19</sup> As **SyCPA 12**, **102**, and **123** are structurally distinct from any previously reported natural products (Figure S2); they provide novel chemical scaffolds for investigating the bioactivity of cationic peptide antibiotics.

**Inhibition of Cell Wall Biosynthesis by SyCPA 4.** Antibiotics that bind cell wall biosynthetic intermediates often result in the accumulation of the lipid II precursor UDP-MurNAc-pentapeptide. On the basis of the spectrum activity of each SyCPA, cultures of either *S. aureus* or *B. subtilis* were exposed to individual SyCPAs and then monitored by LCMS for the accumulation of UDP-MurNAc-pentapeptide (Figure 5a). *B. subtilis* cultures treated with **SyCPA 4** containing increased concentrations of UDP-MurNAc-pentapeptide indicated inhibition of cell biosynthesis by this antibiotic (Figure 5a). **SyCPA 4** was most active against *B. subtilis* in our initial screen. When tested against a broader collection of bacteria it remained most potent against Gram-positive Bacilli (e.g., *Bacillus anthracis*, *Bacillus cereus*, and *Lactobacillus rhamnosus*, Figure 5b) but largely inactive against other strains. The structure of the peptidoglycan in Gram-positive Bacilli differs from that in most other Gram-positive bacteria in that a *meso*-diaminopimelic acid replaces lysine at the third position of the pentapeptide moiety (Figure 5c),<sup>20</sup> suggesting that **SyCPA 4** antibiosis may depend on an

interaction with this divergent residue. Interestingly, Gram-negative peptidoglycan also contains *meso*-diaminopimelic acid; however, **SyCPA 4** was not active against any of the Gram-negative bacteria we initially tested. We expected this might be due to the Gram-negative outer membrane preventing access to the peptidoglycan. We therefore tested the effect of polymyxin, which disrupts the outer membrane of Gram-negative bacteria, on the antibiosis of **SyCPA 4**, as well as the other SyCPAs. As would be expected, all SyCPAs with native activity against Gram-negative bacteria showed increased potency in the presence of polymyxin (Figure 5d). Among the Gram-positive specific SyCPAs, **SyCPA 4** was the only one to show an increased spectrum of activity. In fact, in combination with polymyxin, **SyCPA 4** is active against most Gram-negative ESKAPE pathogens. While detailed binding assays will be required to determine the exact mechanism of **SyCPA 4**'s cell wall inhibition activity, its spectrum of activity suggests that it likely specifically interacts with the *meso*-diaminopimelic acid moiety that is common to the peptidoglycan of Gram-positive Bacilli as well as Gram-negative bacteria.

Interestingly, **SyCPA 4** was also the only Gram-positive specific antibiotic that caused a dramatic increase in SYTOX fluorescence, suggesting that in addition to inhibiting cell wall biosynthesis, it also induces cell lysis (Figure 4c). This is reminiscent of the bifunctional semisynthetic glycolipopeptide telavancin that was recently approved for treatment of antibiotic resistant Gram-positive bacterial infections.<sup>21</sup> In the case of telavancin, the peptide moiety interacts with peptidoglycan to inhibit cell wall biosynthesis and the lipid substituent interacts with the bacterial membrane to cause depolarization. **SyCPA 4** induced an increase in SYTOX

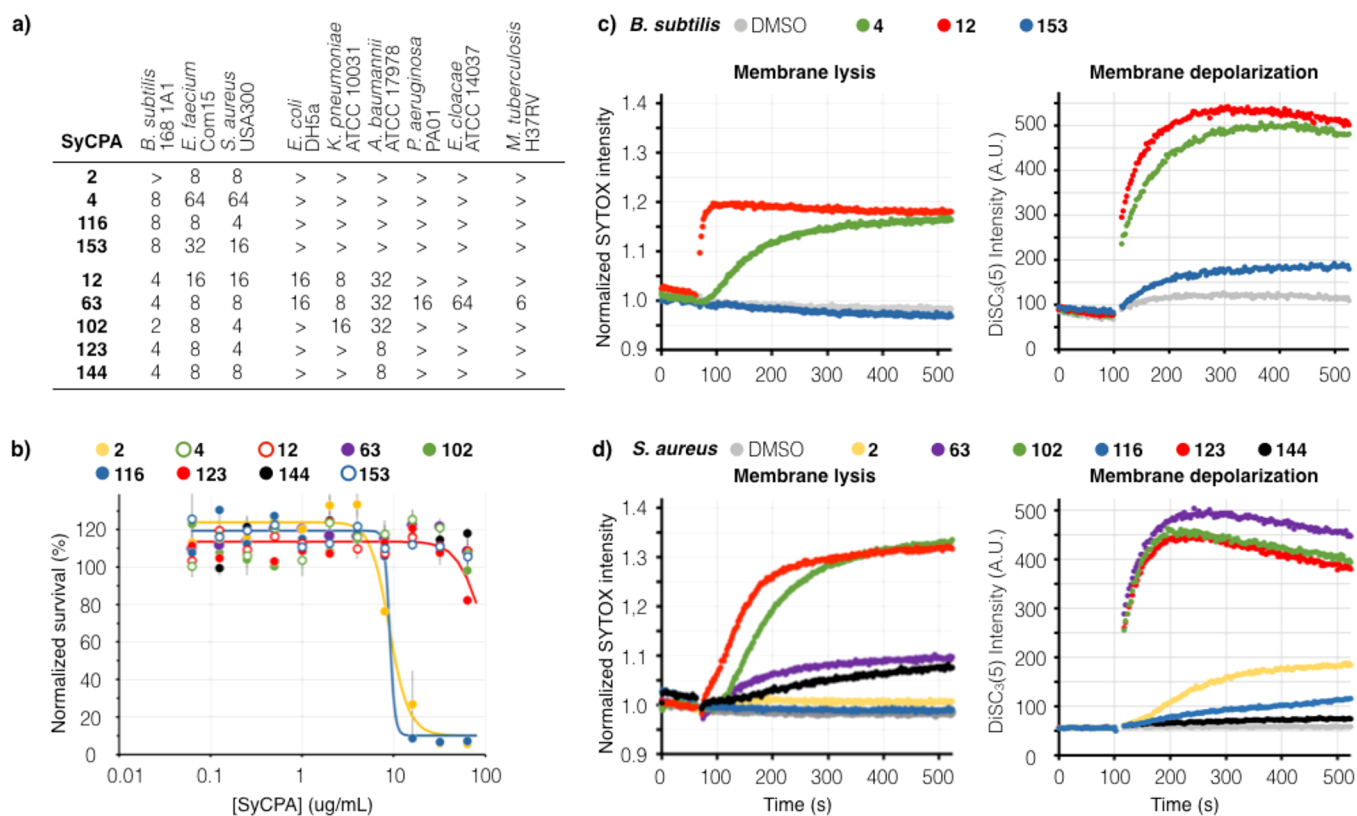


**Figure 4.** (a) Minimum inhibitory concentrations (MICs) of the SyCPAs ( $\mu\text{g/mL}$ , “>” indicates the MIC is greater than  $64 \mu\text{g/mL}$ ; the highest concentration tested for *M. tuberculosis* was  $12.5 \mu\text{g/mL}$ ). (b) Cytotoxicity of *B. subtilis* and *S. aureus* active SyCPAs were assessed using HeLa cells and the MTT metabolic activity assay. Cell survival was normalized to that of the DMSO control. Syn-BNP antibiotics were assayed at  $4\times$  MIC against either (c) *B. subtilis* or (d) *S. aureus*. Two fluorescent dyes were used to probe potential membrane acting mechanisms: SYTOX Green for lysis and DiSC<sub>3</sub>(5) for depolarization. DMSO was used as the negative control in all assays (light gray traces).

fluorescence at  $4\times$  its MIC but had no such effect at  $1\times$  its MIC, suggesting that inhibition of cell wall biosynthesis is likely its principal mode of action, except at very high concentrations. Bifunctional antibiotics are of considerable interest due to the low rates of resistance development they tend to exhibit.<sup>22</sup> This mirrors our experience with SyCPA 4 in that all efforts to raise resistant mutants have so far been unsuccessful. SyCPA 4 was given the trivial name “gladiosyn” (*Burkholderia gladioli* BSR3 syn-BNP).

**Membrane Depolarization and Mycobacterium tuberculosis Growth Inhibition by SyCPA 63.** Cell membrane depolarization was measured using the voltage-sensitive dye 3,3'-dipropylthiadicarbonycyanine iodide (DiSC<sub>3</sub>(5)). In addition to the four SyCPAs that caused cell lysis (SyCPA 4, 12, 102, and 123), one additional antibiotic, SyCPA 63, induced an increase in DiSC<sub>3</sub>(5) fluorescence (Figure 5), indicating that it depolarizes the bacterial membrane but does not lyse bacteria. SyCPA 63 shows the broadest spectrum of activity among the SyCPAs we identified. Among the Gram-negative bacteria we tested, it was most active against *K. pneumoniae* ( $8 \mu\text{g/mL}$ ) but also showed modest antibacterial activity against most of the Gram-negative bacteria in our panel. Interestingly, when tested for activity against other pathogens, SyCPA 63 was the only SyCPA that inhibited the growth of *M. tuberculosis* H37Rv (MIC  $6 \mu\text{g/mL}$ ) (Figure 4a). SyCPA 63's broad spectrum of activity against diverse pathogens, together with its minimal HeLa cell cytotoxicity and our failure to identify SyCPA 63 resistant mutants in laboratory experiments, make it an appealing structure for future synthetic

efforts designed to improve its potency. We have given SyCPA 63 the trivial name thurinsyn (*Bacillus thuringiensis* BMB171 syn-BNP).

**Resistant Mutant Screening.** To look for other potential mechanisms of action, we attempted to raise resistant mutants for each antibiotic that did not strongly respond to any of the discrete assays we used above (SyCPAs 2, 116, 144, and 153).

**Dysregulation of the ClpP Protease by SyCPA 116.** In an initial round of resistant mutant screening using *S. aureus* USA 300, all SyCPA 116 resistant mutants contained single-nucleotide polymorphisms (SNPs) in the *farR* gene (Table S4). FarR is a LysR transcription factor that induces expression of FarE, an efflux pump that has been associated with resistance to antimicrobial fatty acids.<sup>23</sup> Constitutive overexpression of the *farER* efflux system (pALC<sub>farER</sub>) in an *S. aureus* *farER* deletion mutant<sup>23</sup> (SyCPA 116 MIC of  $8 \mu\text{g/mL}$ ) conferred resistance to SyCPA 116 (MIC  $> 64 \mu\text{g/mL}$ ), suggesting that FarE can efflux SyCPA 116. Therefore, in a second round of screening, we attempted to raise resistant mutants using the *farER* deletion strain. This yielded mutants that were able to grow on  $>128 \mu\text{g/mL}$  of SyCPA 116. Whole genome sequencing of these strains identified mutants with SNPs in the ClpP protease (*clpP*) gene or in an operon that encodes a multisubunit Na<sup>+</sup>/H<sup>+</sup> antiporter that has been associated with tolerance to diverse molecules including salt, cholate, and thrombin-induced platelet microbicidal protein.<sup>24</sup> Interestingly, a number of the *clpP* point mutations introduced stop codons (Figure 6a), which suggested that disruption of this protease provides resistance to SyCPA 116. This

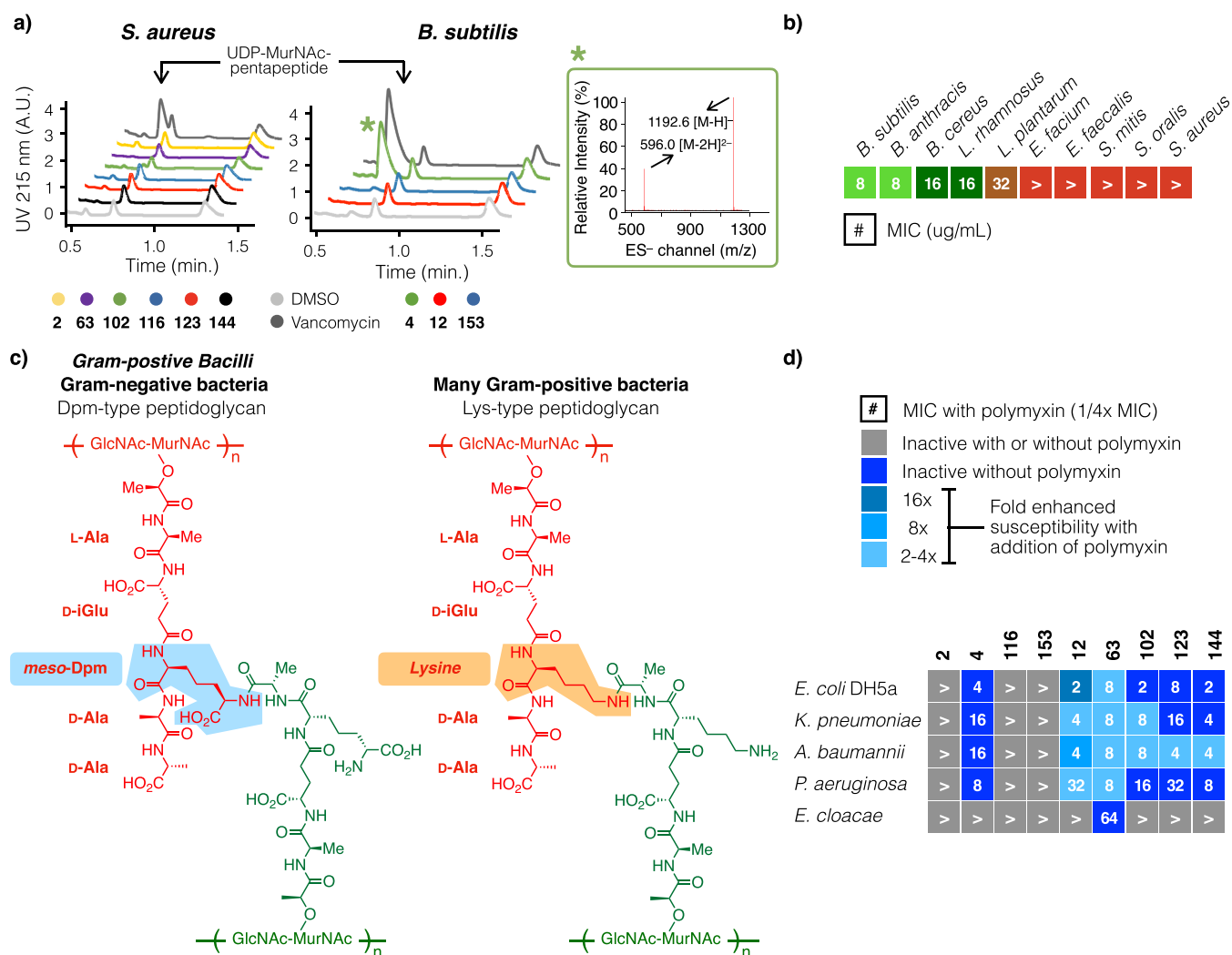


**Figure 5.** (a) All peptides were tested at 20  $\mu\text{g}/\text{mL}$  for inducing the accumulation of the lipid II biosynthetic precursor UDP-MurNAc-pentapeptide. Vancomycin and DMSO were used as the positive and negative controls, respectively (dark and light gray traces). (b) SyCPA 4 (gladiosyn) is most active against Gram-positive Bacilli. (c) *Bacillus* and Gram-negative bacteria use *meso*-diaminopimelic acid to cross-link their peptidoglycans in cell wall biosynthesis, as opposed to using lysine in those of other Gram-positive bacteria. (d) SyCPAs show improved activities when tested in combination with polymyxin at 1/4x MIC of each respective bacterium ( $\mu\text{g}/\text{mL}$ , ">" indicates the MIC is greater than 64  $\mu\text{g}/\text{mL}$ ).

hypothesis was confirmed by the fact that a targeted *clpP* deletion mutant (*S. aureus* SH1000  $\Delta\text{clpP}$ ) was resistant to SyCPA 116 (>128  $\mu\text{g}/\text{mL}$ ) but the parent of this strain was not.<sup>25</sup>

The ClpP protease is part of a protein degradation machinery that targets misfolded and unneeded proteins.<sup>26</sup> This system is not essential to *S. aureus*. Inhibition of ClpP is therefore not a viable antibacterial mode of action. On the other hand, dysregulation of ClpP that results in uncontrolled protein degradation is known to be lethal (Figure 6b).<sup>27</sup> The fact that deletion of *clpP* provides resistance suggests a ClpP dysregulation mode of action for SyCPA 116. To the best of our knowledge, only one known family of bacterial natural product antibiotics, the acyl depsipeptides (ADEPs), functions by dysregulating ClpP.<sup>27,28</sup> Although both SyCPA 116 and the ADEPs are cyclic acylated peptides, their structures are quite different (Figure 6c): (1) they share no amino acids, (2) their macrocycles differ in size, (3) SyCPA 116 is not a depsipeptide but instead cyclized through an amide bond, and (4) the N-terminus of SyCPA 116 contains a fully saturated acyl substituent, while ADEPs contain polyunsaturated acyl

substituents. Whether ADEPs and SyCPA 116 bind the same site or even function by the exact same mechanism remains to be determined. Efforts to identify unique chemical matter that activates ClpP and kills bacteria have seen only modest success.<sup>29</sup> As seen with some ADEP analogs, SyCPA 116 also shows human cell line toxicity (Figure 4b). This is likely due to dysregulation of the mitochondrial ClpP protease, which is known to lead to apoptotic cell death.<sup>30</sup> The SyCPA 116 scaffold therefore provides opportunities to explore ClpP protease activation not only as an antibacterial mode of action but also as a way of killing cancer cells. We have given SyCPA 116 the name "collimosyn" (*Collimonas fungivorans* Ter331 syn-BNP).

**SyCPAs 2, 144, and 153.** SyCPAs 2, 144, and 153 were neither highly active in any of the discrete assays we looked at initially nor were we able to identify resistant mutants that could provide insight into their modes of action. Each of these antibiotics did cause a slight increase in either SYTOX or DiSC<sub>3</sub>(5) fluorescence in our initial assays (Figure 4c,d), suggesting limited cell lysis or membrane depolarization, respectively. Additional experiments will be required to



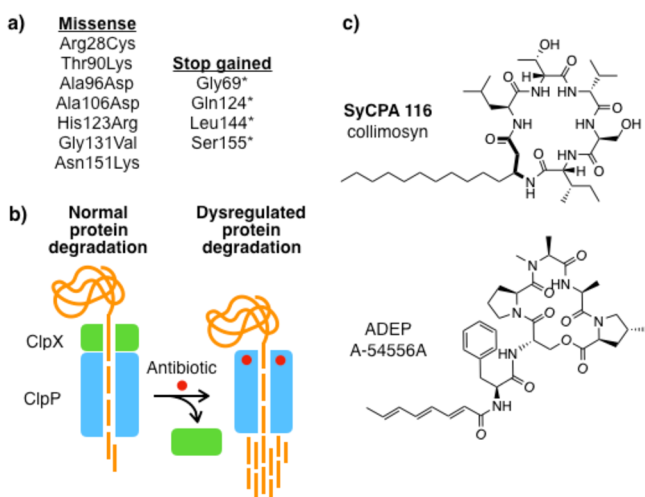


**Figure 6.** (a) Mutations in *clpP* that conferred resistance to SyCPA 116 (collimosyn). (b) Dysregulation of ClpP results in uncontrolled protein degradation which is lethal to *S. aureus*. (c) Comparison of SyCPA 116 (collimosyn) and ADEP structures.

determine if this is indicative of the antibiotic's primary mode of action or whether this is a secondary effect. Although their modes of action remain to be determined, among these antibiotics, SyCPA 144 is of particular interest for future synthetic optimization studies due to its native activity against *A. baumannii*, broad spectrum activity in the presence of polymyxin, lack of toxicity to human cells *in vitro*, and our inability to raise resistance mutants in laboratory-based experiments using either Gram-positive or Gram-negative bacteria (*S. aureus*, *B. subtilis*, and *Escherichia coli imp*). We have named SyCPA 144 "mucilasyne" (*Paenibacillus mucilaginosus* syn-BNP).

## CONCLUSION

Continuous improvement in DNA sequencing technologies promises to uncover an increasingly large number of uncharacterized bacterial biosynthetic gene clusters. The biosynthetic instructions contained in these gene clusters encode a reservoir of naturally occurring bioactivities including the diverse mechanisms that bacteria have evolved to control the growth of other bacteria. The successful translation of uncharacterized biosynthetic gene clusters into bioactive molecules should have a significant positive impact on antibiotic discovery pipelines and in turn on our ability to address the growing problem of antimicrobial resistance. Of the 96 gene clusters we explored using the syn-BNP approach, almost ten percent inspired the synthesis of an antibiotic with activity against antibiotic-resistant pathogens of clinical interest, many of which failed to develop resistance in laboratory experiments. Our data suggest that these new antibiotics function by multiple different modes of action.

The syn-BNP peptides reported range from 5 to 14 amino acids in length with the median length being 7 amino acids. To cover all possible 7-mer peptide sequences composed of the canonical amino acids in both D- and L-forms calls for a combinatorial library that contains  $\sim 1.6 \times 10^{11}$  members. A library of this size is unrealistic to build or screen with currently available methods. The syn-BNP approach takes cues from evolution to narrow our scale of synthesis and increases the likelihood of identifying bioactive compounds. Syn-BNPs

are not expected to represent perfect translations of the instructions contained in gene clusters but instead biosynthetically inspired structures with enough similarity to native metabolites to capture the diverse bioactivities encoded by uncharacterized gene clusters.

In fact, because the vast majority of biosynthetic gene clusters are silent in laboratory conditions, it is not currently possible to determine the exact product of most biosynthetic gene clusters that inspire syn-BNPs. As has often been done with traditional natural products, we expect mechanistically interesting syn-BNPs will serve as inspiration for the generation of more potent and clinically relevant small molecule derivatives in subsequent synthetic optimization studies. The work outlined here adds to a growing body of evidence that the syn-BNP approach represents an effective, scalable, and orthogonal method for using the biosynthetic instructions found in natural product biosynthetic gene clusters to inspire the creation of bioactive small molecules. Building on our previous work involving largely linear syn-BNP peptides, this study expands to the design and synthesis of our largest collection yet of cyclic syn-BNP peptides. Subsequent screening and mechanistic studies show that this approach is particularly fruitful in the discovery of antibiotics with diverse modes of action. Improvements in bioinformatic algorithms for predicting chemical structures from biosynthetic gene clusters together with the incorporation of additional synthetic complexity beyond peptide cyclization will undoubtedly lead to even higher hit rates and more diverse bioactivities in future syn-BNP studies.

## ASSOCIATED CONTENT

### Supporting Information

The Supporting Information is available free of charge at <https://pubs.acs.org/doi/10.1021/jacs.0c04376>.

List of syn-BNP peptides, microbial strain information, analytical data (HRMS, MS/MS, and  $^1\text{H}$  NMR), SNPs of resistant mutants, biosynthetic gene clusters of SyCPAs (PDF)

## AUTHOR INFORMATION

### Corresponding Author

Sean F. Brady – Laboratory of Genetically Encoded Small Molecules, The Rockefeller University, New York, New York 10065, United States; Email: [sbrady@mail.rockefeller.edu](mailto:sbrady@mail.rockefeller.edu)

### Authors

John Chu – Laboratory of Genetically Encoded Small Molecules, The Rockefeller University, New York, New York 10065, United States; [orcid.org/0000-0002-7033-7229](https://orcid.org/0000-0002-7033-7229)

Bimal Koirala – Laboratory of Genetically Encoded Small Molecules, The Rockefeller University, New York, New York 10065, United States; [orcid.org/0000-0003-1806-7935](https://orcid.org/0000-0003-1806-7935)

Nicholas Forelli – Laboratory of Genetically Encoded Small Molecules, The Rockefeller University, New York, New York 10065, United States

Xavier Vila-Farres – Laboratory of Genetically Encoded Small Molecules, The Rockefeller University, New York, New York 10065, United States

Melinda A. Ternei – Laboratory of Genetically Encoded Small Molecules, The Rockefeller University, New York, New York 10065, United States

**Thahmina Ali** – Laboratory of Genetically Encoded Small Molecules, The Rockefeller University, New York, New York 10065, United States

**Dominic A. Colosimo** – Laboratory of Genetically Encoded Small Molecules, The Rockefeller University, New York, New York 10065, United States

Complete contact information is available at:  
<https://pubs.acs.org/10.1021/jacs.0c04376>

## Funding

This work was supported by NIH (Project Nos. 1U19AI142731 and 5R35GM122559).

## Notes

The authors declare no competing financial interest.

## ACKNOWLEDGMENTS

We thank the Fischetti (*K. pneumoniae*, *A. baumannii*, *B. anthracis*), Hang (*E. faecium*), McGavin (*S. aureus* USA300  $\Delta$ farER), and Cheung (*S. aureus* SH1000 and SH1000  $\Delta$ ClpP) laboratories for providing strains and plasmids. We also thank the High Throughput Screening and Spectroscopy Resource Center at the Rockefeller University for support in obtaining analytical data (HRMS).

## ABBREVIATIONS

MIC, minimum inhibitory concentration; NRP, nonribosomal peptide; NRPS, nonribosomal peptide synthetase; syn-BNP, synthetic-bioinformatic natural product; SyCPA, syn-BNP cyclic peptide antibiotics

## REFERENCES

- (1) Newman, D. J.; Cragg, G. M. Natural products as sources of new drugs from 1981 to 2014. *J. Nat. Prod.* **2016**, *79*, 629.
- (2) Walsh, C. T. *Antibiotics: actions, origins, resistance*; ASM Press: Washington, DC, 2003.
- (3) (a) Staley, J. T.; Konopka, A. Measurement of in situ activities of nonphotosynthetic microorganisms in aquatic and terrestrial habitats. *Annu. Rev. Microbiol.* **1985**, *39*, 321. (b) Jensen, P. R. Natural products and the gene cluster revolution. *Trends Microbiol.* **2016**, *24*, 968. (c) Libis, V.; Antonovsky, N.; Zhang, M.; Shang, Z.; Montiel, D.; Maniko, J.; Ternei, M. A.; Calle, P. Y.; Lemetre, C.; Owen, J. G.; Brady, S. F. Uncovering the biosynthetic potential of rare metagenomic DNA using co-occurrence network analysis of targeted sequences. *Nat. Commun.* **2019**, *10*, 3848.
- (4) Blin, K.; Medema, M. H.; Kottmann, R.; Lee, S. Y.; Weber, T. The antiSMASH database, a comprehensive database of microbial secondary metabolite biosynthetic gene clusters. *Nucleic Acids Res.* **2017**, *45*, D555.
- (5) (a) Handelsman, J.; Rondon, M. R.; Brady, S. F.; Clardy, J.; Goodman, R. M. Molecular biological access to the chemistry of unknown soil microbes: a new frontier for natural products. *Chem. Biol.* **1998**, *5*, R245. (b) Charlop-Powers, Z.; Milshteyn, A.; Brady, S. F. Metagenomic small molecule discovery methods. *Curr. Opin. Microbiol.* **2014**, *19*, 70. (c) Kalkreuter, E.; Pan, G.; Cepeda, A. J.; Shen, B. Targeting bacterial genomes for natural product discovery. *Trends Pharmacol. Sci.* **2020**, *41*, 13.
- (6) (a) Chu, J.; Vila-Farres, X.; Inoyama, D.; Ternei, M.; Cohen, L. J.; Gordon, E. A.; Reddy, B. V.; Charlop-Powers, Z.; Zebroski, H. A.; Gallardo-Macias, R.; Jaskowski, M.; Satish, S.; Park, S.; Perlin, D. S.; Freundlich, J. S.; Brady, S. F. Discovery of MRSA active antibiotics using primary sequence from the human microbiome. *Nat. Chem. Biol.* **2016**, *12*, 1004. (b) Vila-Farres, X.; Chu, J.; Inoyama, D.; Ternei, M. A.; Lemetre, C.; Cohen, L. J.; Cho, W.; Reddy, B. V.; Zebroski, H. A.; Freundlich, J. S.; Perlin, D. S.; Brady, S. F. Antimicrobials inspired by nonribosomal peptide synthetase gene clusters. *J. Am. Chem. Soc.*

**2017**, *139*, 1404. (c) Vila-Farres, X.; Chu, J.; Ternei, M. A.; Lemetre, C.; Park, S.; Perlin, D. S.; Brady, S. F. An optimized synthetic-bioinformatic natural product antibiotic sterilizes multidrug-resistant *Acinetobacter baumannii*-infected wounds. *mSphere* **2018**, *3*, No. e00528–17. (d) Chu, J.; Vila-Farres, X.; Inoyama, D.; Gallardo-Macias, R.; Jaskowski, M.; Satish, S.; Freundlich, J. S.; Brady, S. F. Human microbiome inspired antibiotics with improved beta-lactam synergy against MDR *Staphylococcus aureus*. *ACS Infect. Dis.* **2018**, *4*, 33. (e) Chu, J.; Vila-Farres, X.; Brady, S. F. Bioactive synthetic-bioinformatic natural product cyclic peptides inspired by nonribosomal peptide synthetase gene clusters from the human microbiome. *J. Am. Chem. Soc.* **2019**, *141*, 15737.

(7) Fischbach, M. A.; Walsh, C. T. Assembly-line enzymology for polyketide and nonribosomal peptide antibiotics: logic, machinery, and mechanisms. *Chem. Rev.* **2006**, *106*, 3468.

(8) Blin, K.; Medema, M. H.; Kazempour, D.; Fischbach, M. A.; Breitling, R.; Takano, E.; Weber, T. antiSMASH 2.0: a versatile platform for genome mining of secondary metabolite producers. *Nucleic Acids Res.* **2013**, *41*, W204.

(9) Weinstein, M. P. *Methods for dilution antimicrobial susceptibility tests for bacteria that grow aerobically*, 9th ed.; Clinical and Laboratory Standards Institute: Wayne, PA, 2012.

(10) (a) Stachelhaus, T.; Mootz, H. D.; Marahiel, M. A. The specificity-conferring code of adenylation domains in nonribosomal peptide synthetases. *Chem. Biol.* **1999**, *6*, 493. (b) Minowa, Y.; Araki, M.; Kanehisa, M. Comprehensive analysis of distinctive polyketide and nonribosomal peptide structural motifs encoded in microbial genomes. *J. Mol. Biol.* **2007**, *368*, 1500. (c) Rottig, M.; Medema, M. H.; Blin, K.; Weber, T.; Rausch, C.; Kohlbacher, O. NRPSpredictor2: a web server for predicting NRPS adenylation domain specificity. *Nucleic Acids Res.* **2011**, *39*, W362.

(11) *Genome List - Genome*; NCBI, 2014. <https://www.ncbi.nlm.nih.gov/genome/browse#!/overview/> (accessed 12-2014).

(12) Horsman, M. E.; Hari, T. P.; Boddy, C. N. Polyketide synthase and non-ribosomal peptide synthetase thioesterase selectivity: logic gate or a victim of fate? *Nat. Prod. Rep.* **2016**, *33*, 183.

(13) (a) *Dictionary of Natural Products*; CRC Press, 2020. <http://dnp.chemnetbase.com/faces/chemical/ChemicalSearch.xhtml> (accessed 04-10-2020). (b) Medema, M. H.; Kottmann, R.; Yilmaz, P.; Cummings, M.; Biggins, J. B.; Blin, K.; de Bruijn, I.; Chooi, Y. H.; Claesen, J.; Coates, R. C.; Cruz-Morales, P.; Duddela, S.; Dusterhus, S.; Edwards, D. J.; Fewer, D. P.; Garg, N.; Geiger, C.; Gomez-Escribano, J. P.; Greule, A.; Hadjithomas, M.; Haines, A. S.; Helfrich, E. J.; Hillwig, M. L.; Ishida, K.; Jones, A. C.; Jones, C. S.; Jungmann, K.; Kegler, C.; Kim, H. U.; Kotter, P.; Krug, D.; Masschelein, J.; Melnik, A. V.; Mantovani, S. M.; Monroe, E. A.; Moore, M.; Moss, N.; Nutzmann, H. W.; Pan, G.; Pati, A.; Petras, D.; Reen, F. J.; Rosconi, F.; Rui, Z.; Tian, Z.; Tobias, N. J.; Tsunematsu, Y.; Wiemann, P.; Wyckoff, E.; Yan, X.; Yim, G.; Yu, F.; Xie, Y.; Aigle, B.; Apel, A. K.; Balibar, C. J.; Balskus, E. P.; Barona-Gomez, F.; Bechthold, A.; Bode, H. B.; Borriss, R.; Brady, S. F.; Brakhage, A. A.; Caffrey, P.; Cheng, Y. Q.; Clardy, J.; Cox, R. J.; De Mot, R.; Donadio, S.; Donia, M. S.; van der Donk, W. A.; Dorrestein, P. C.; Doyle, S.; Driessen, A. J.; Ehling-Schulz, M.; Entian, K. D.; Fischbach, M. A.; Gerwick, L.; Gerwick, W. H.; Gross, H.; Gust, B.; Hertweck, C.; Hofte, M.; Jensen, S. E.; Ju, J.; Katz, L.; Kaysser, L.; Klassen, J. L.; Keller, N. P.; Kormanec, J.; Kuipers, O. P.; Kuzuyama, T.; Kyrpides, N. C.; Kwon, H. J.; Lautru, S.; Lavigne, R.; Lee, C. Y.; Lincun, B.; Liu, X.; Liu, W.; Luzhetskyy, A.; Mahmud, T.; Mast, Y.; Mendez, C.; Metsa-Ketela, M.; Micklefield, J.; Mitchell, D. A.; Moore, B. S.; Moreira, L. M.; Muller, R.; Neilan, B. A.; Nett, M.; Nielsen, J.; O'Gara, F.; Oikawa, H.; Osburne, A.; Osburne, M. S.; Ostash, B.; Payne, S. M.; Pernodet, J. L.; Petricek, M.; Piel, J.; Ploux, O.; Raaijmakers, J. M.; Salas, J. A.; Schmitt, E. K.; Scott, B.; Seipke, R. F.; Shen, B.; Sherman, D. H.; Sivonen, K.; Smanski, M. J.; Sosio, M.; Stegmann, E.; Sussmuth, R. D.; Tahlan, K.; Thomas, C. M.; Tang, Y.; Truman, A. W.; Viaud, M.; Walton, J. D.; Walsh, C. T.; Weber, T.; van Wezel, G. P.; Wilkinson, B.; Willey, J. M.; Wohlleben, W.; Wright, G. D.; Ziemert, N.; Zhang, C.; Zotchev, S. B.; Breitling,

R.; Takano, E.; Glockner, F. O. Minimum information about a biosynthetic gene cluster. *Nat. Chem. Biol.* **2015**, *11*, 625.

(14) Walsh, C. T. Polyketide and nonribosomal peptide antibiotics: modularity and versatility. *Science* **2004**, *303*, 1805.

(15) Boucher, H. W.; Talbot, G. H.; Bradley, J. S.; Edwards, J. E.; Gilbert, D.; Rice, L. B.; Scheld, M.; Spellberg, B.; Bartlett, J. Bad bugs, no drugs: no ESCAPE! An update from the Infectious Diseases Society of America. *Clin. Infect. Dis.* **2009**, *48*, 1.

(16) *SciFinder: A CAS solution*; American Chemical Society, 2020. <https://scifinder.cas.org/> (accessed 01-2020).

(17) Lambert, P. A.; Allison, D. G.; Gilbert, P. Antibiotics that act on the cell wall and membrane. *Mol. Med. Microbiol.* **2002**, *1*, 591.

(18) Eband, R. M.; Walker, C.; Eband, R. F.; Magarvey, N. A. Molecular mechanisms of membrane targeting antibiotics. *Biochim. Biophys. Acta, Biomembr.* **2016**, *1858*, 980.

(19) Lazar, V.; Martins, A.; Spohn, R.; Daruka, L.; Grezal, G.; Fekete, G.; Szamel, M.; Jangir, P. K.; Kintszes, B.; Csorgo, B.; Nyerges, A.; Gyorki, A.; Kincses, A.; Der, A.; Walter, F. R.; Deli, M. A.; Urban, E.; Hegedus, Z.; Olajos, G.; Mehi, O.; Balint, B.; Nagy, I.; Martinek, T. A.; Papp, B.; Pal, C. Antibiotic-resistant bacteria show widespread collateral sensitivity to antimicrobial peptides. *Nat. Microbiol.* **2018**, *3*, 718.

(20) Firczuk, M.; Bochtler, M. Folds and activities of peptidoglycan amidases. *FEMS Microbiol. Rev.* **2007**, *31*, 676.

(21) Higgins, D. L.; Chang, R.; Debabov, D. V.; Leung, J.; Wu, T.; Krause, K. M.; Sandvik, E.; Hubbard, J. M.; Kaniga, K.; Schmidt, D. E., Jr.; Gao, Q.; Cass, R. T.; Karr, D. E.; Benton, B. M.; Humphrey, P. P. Telavancin, a multifunctional lipoglycopeptide, disrupts both cell wall synthesis and cell membrane integrity in methicillin-resistant *Staphylococcus aureus*. *Antimicrob. Agents Chemother.* **2005**, *49*, 1127.

(22) Pokrovskaya, V.; Baasov, T. Dual-acting hybrid antibiotics: a promising strategy to combat bacterial resistance. *Expert Opin. Drug Discovery* **2010**, *5*, 883.

(23) Alnaseri, H.; Kuiack, R. C.; Ferguson, K. A.; Schneider, J. E. T.; Heinrichs, D. E.; McGavin, M. J. DNA binding and sensor specificity of FarR, a novel TetR family regulator required for induction of the fatty acid efflux pump FarE in *Staphylococcus aureus*. *J. Bacteriol.* **2019**, *201*, 201.

(24) (a) Bayer, A. S.; McNamara, P.; Yeaman, M. R.; Lucindo, N.; Jones, T.; Cheung, A. L.; Sahl, H. G.; Proctor, R. A. Transposon disruption of the complex I NADH oxidoreductase gene (snoD) in *Staphylococcus aureus* is associated with reduced susceptibility to the microbicidal activity of thrombin-induced platelet microbicidal protein 1. *J. Bacteriol.* **2006**, *188*, 211. (b) Sannasiddappa, T. H.; Hood, G. A.; Hanson, K. J.; Costabile, A.; Gibson, G. R.; Clarke, S. R. *Staphylococcus aureus* MnhF mediates cholerae efflux and facilitates survival under human colonic conditions. *Infect. Immun.* **2015**, *83*, 2350. (c) Vaish, M.; Price-Whelan, A.; Reyes-Robles, T.; Liu, J.; Jereen, A.; Christie, S.; Alonzo, F., 3rd; Benson, M. A.; Torres, V. J.; Krulwich, T. A. Roles of *Staphylococcus aureus* Mnh1 and Mnh2 antiporters in salt tolerance, alkali tolerance, and pathogenesis. *J. Bacteriol.* **2018**, *200*, No. e00611–17.

(25) Frees, D.; Qazi, S. N.; Hill, P. J.; Ingmer, H. Alternative roles of ClpX and ClpP in *Staphylococcus aureus* stress tolerance and virulence. *Mol. Microbiol.* **2003**, *48*, 1565.

(26) Clarke, A. K. Variations on a theme: combined molecular chaperone and proteolysis functions in Clp/HSP100 proteins. *J. Biosci.* **1996**, *21*, 161.

(27) Kirstein, J.; Hoffmann, A.; Lilie, H.; Schmidt, R.; Rubsam-Waigmann, H.; Brotz-Oesterhelt, H.; Mogk, A.; Turgay, K. The antibiotic ADEP reprogrammes ClpP, switching it from a regulated to an uncontrolled protease. *EMBO Mol. Med.* **2009**, *1*, 37.

(28) Hinzen, B.; Raddatz, S.; Paulsen, H.; Lampe, T.; Schumacher, A.; Habich, D.; Hellwig, V.; Benet-Buchholz, J.; Endermann, R.; Labischinski, H.; Brotz-Oesterhelt, H. Medicinal chemistry optimization of acyldepsipeptides of the enopeptin class antibiotics. *ChemMedChem* **2006**, *1*, 689.

(29) (a) Leung, E.; Datti, A.; Cossette, M.; Goodreid, J.; McCaw, S. E.; Mah, M.; Nakhamchik, A.; Ogata, K.; El Bakkouri, M.; Cheng, Y.

Q.; Wodak, S. J.; Eger, B. T.; Pai, E. F.; Liu, J.; Gray-Owen, S.; Batey, R. A.; Houry, W. A. Activators of cylindrical proteases as antimicrobials: identification and development of small molecule activators of ClpP protease. *Chem. Biol.* **2011**, *18*, 1167. (b) Lavey, N. P.; Coker, J. A.; Ruben, E. A.; Duerfeldt, A. S. Sclerotamide: the first non-peptide-based natural product activator of bacterial caseinolytic protease P. *J. Nat. Prod.* **2016**, *79*, 1193. (c) Ye, F.; Li, J.; Yang, C. G. The development of small-molecule modulators for ClpP protease activity. *Mol. Biosyst.* **2017**, *13*, 23.

(30) Wong, K. S.; Mabanglo, M. F.; Seraphim, T. V.; Mollica, A.; Mao, Y. Q.; Rizzolo, K.; Leung, E.; Moutaoufik, M. T.; Hoell, L.; Phanse, S.; Goodreid, J.; Barbosa, L. R. S.; Ramos, C. H. I.; Babu, M.; Mennella, V.; Batey, R. A.; Schimmer, A. D.; Houry, W. A. Acyldepsipeptide analogs dysregulate human mitochondrial ClpP protease activity and cause apoptotic cell death. *Cell Chem. Biol.* **2018**, *25*, 1017.